Distinct Roles of the *Drosophila ninaC* Kinase and Myosin Domains Revealed by Systematic Mutagenesis

Jeffery A. Porter and Craig Montell

Department of Biological Chemistry and Department of Neuroscience, The Johns Hopkins University School of Medicine, Baltimore, Maryland 21205

Abstract. The *Drosophila ninaC* locus encodes a rhabdomere specific protein (p174) with linked protein kinase and myosin domains, required for a wild-type ERG and to prevent retinal degeneration. To investigate the role for linked kinase and myosin domains, we analyzed mutants generated by site-directed mutagenesis. Mutation of the kinase domain resulted in an ERG phenotype but no retinal degeneration. Deletion of the myosin domain caused a change in the subcellular distribution of p174 and resulted in both ERG and retinal degeneration phenotypes. Temperature-sensitive mutations in the myosin domain resulted in retinal degeneration, but no ERG phenotype. These results indicated that the ERG and retinal degeneration phenotypes were not strictly coupled suggesting that the myosin domain has multiple functions. We propose that the role of the kinase domain is to regulate other rhabdomeric proteins important in phototransduction and that the myosin domain has at least two roles: to traffic the kinase into the rhabdomeres and to maintain the rhabdomeres.

THE *Drosophila ninaC* proteins (NINAC) are chimeric proteins consisting of linked protein kinase and myosin head domains. Protein kinases are regulatory molecules that modulate the activities of other proteins by phosphorylation. Protein phosphorylation has been shown to be important in regulating proteins required in a wide diversity of processes including the cell cycle, differentiation, cell movement, and sensory transduction (reviewed in Edelman et al., 1987; Cohen, 1989; Norbury and Nurse, 1992. Tan et al., 1992). Myosins are motor molecules which contain an approximately 800 amino acid head domain required for ATP-dependent translocation along actin filaments. The best characterized myosins, referred to as conventional myosins or myosin-IIs, are filament forming double-headed molecules, found in muscle as well as non-muscle cells (reviewed in Warrick and Spudich, 1987; Korn and Hammer, 1988). The head domain in conventional myosins or myosin IIs is joined to an α-helical COOH-terminal tail which is typically approximately 1,000 amino acids. Unconventional myosins are a diverse group of non-filament forming mostly single-headed molecules found in a large variety of cell types (reviewed in Pollard et al., 1991; Cheney and Mooseker, 1992; Endow and Titus, 1992). The best-characterized unconventional myosins, myosin-Is, contain non-α-helical tails of about 500 amino acids (reviewed in Pollard et al., 1991; Cheney and Mooseker, 1992). In addition to muscle contraction, myosins have been implicated in organelle movement, cytokinesis, movement of membrane proteins, changes in cell shape, and chemotaxis (reviewed in Spudich, 1989). Although the functions of many protein kinases and myosin IIs have been previously described, the physiological role of a fused putative protein kinase and putative myosin is not clear.

The *ninaC* locus encodes two photoreceptor specific proteins, p174 and p132, both of which contain an NH_2-terminal protein kinase domain joined to a domain homologous to the head region of a myosin heavy chain (Montell and Rubin, 1988). The NINAC proteins are structurally distinct from all known myosins most notably in the presence of the NH_2-terminal protein kinase domain. The two NINAC isoforms differ in the COOH-terminal 420 and 54 amino acid tails unique to p174 and p132, respectively. The p174 protein is localized exclusively to the rhabdomeres and p132 to the cell body (Porter et al., 1992). This indicates that the p174-specific tail domain is required for localization to the rhabdomeres, the microvillar structure which is the site of action of many of the initial steps of phototransduction.

Two phenotypes are associated with mutations in *ninaC*. Null mutations result in an electrophysiological phenotype suggesting that the *ninaC* locus functions in phototransduction (Porter et al., 1992). In addition, *ninaC* photoreceptor cells undergo light and age-dependent retinal degeneration (Matsumoto et al., 1987; Porter et al., 1992). The p174 protein, but not p132, is required for both wild-type electrophysiology and to prevent retinal degeneration (Porter et al., 1992). The phenotypes associated with p174 could be due to disruption of two distinct functions. Alternatively, p174 could have one role and the two phenotypes are obligatorily coupled.

To characterize the functions of the *ninaC* protein kinase

and myosin domains, we constructed and analyzed the effects of 24 site-specific mutations in *ninaC* in vivo. We found that the retinal degeneration and electrophysiological phenotypes were not obligatorily coupled. Deletion of the kinase domain resulted only in an electrophysiological phenotype and deletion of the myosin domain caused mislocalization of the altered p174, retinal degeneration and an electrophysiological phenotype. Among the collection of point mutations in the myosin domain were two that caused temperature-sensitive phenotypes characterized by mislocalization of p174, retinal degeneration and no electrophysiological phenotype. The results of this analysis indicated that the *ninaC* kinase domain had a role in phototransduction and the myosin domain was multifunctional, with roles in phototransduction and in maintaining the rhabdomeres.

Materials and Methods

Construction of Transformant Lines with Mutations in the Kinase and Myosin Domains

The mutations in the kinase and myosin domains were generated by oligonucleotide-directed mutagenesis, using single-stranded pBSXX1 DNA, as described (Porter et al., 1992). pBSXX1 consists of a XbaI-XhoI fragment (coordinates 6.2–10.2 on the *ninaC* genomic map; Montell and Rubin, 1988) subcloned into pBluescriptKS$^+$ (Porter et al., 1992). After mutagenesis, with 21 of the 24 primers, the entire 4.0-kb XhoI-XbaI fragment was sequenced confirming that there were no adventitious mutations in any of these plasmids. The entire 4.0-kb insert in pBSXX1 was not sequenced following mutagenesis with the final three primers used, KATP1, MATP1, and MD, since we did not detect any unintended mutations among the first 21 mutated vectors. The mutated XhoI-XbaI fragments were subsequently subcloned into the ry^+ P element transformation vector, pDM30 (Mismer and Rubin, 1987), as described (Porter et al., 1992). The mutagenized *ninaC* DNAs (400 mg/ml) and pπ25.7 (100 mg/ml) were injected into ~300 $ninaC^{P235}$; *ry* M cytotype embryos as described (Spradling and Rubin, 1982; Rubin and Spradling, 1982). Several independent ry^+ transformants were obtained for each and stocks homozygous for the insertions were generated.

Three oligonucleotide primers were used to construct two large and one small deletion as described in Fig. 1. Nucleotides underlined, in each primer, correspond to the bases flanking the deleted sequence. Preceding each of the following primers are the names of the oligonucleotides used to construct the mutations listed in figure 1: KD, CGGATCCTACGGATAAATTCCTCATCGAAACGAGGACGA; MD, GGTTTCGATGAGAAGCCGGAATATGAGCTGCAGGTGAAGAA; 9, AGCCAGAATGCAGTGCACTTCGTT.

21-oligonucleotide primers were used to construct the point mutations described in Fig. 1. In most cases, the altered amino acid was encoded by the preferred *Drosophila* codon (Aota et al., 1988). Underlined nucleotides correspond to the bases altered by the mutagenesis. The names of the following primers, used to generate the mutations listed in Fig. 1, precede the sequence of the primer: KX, CGTTGCCCTGATGATTCAGCAC; 1, CAGTTTCATTCGCGATATCC; 2, GCTGGAGAAATCATGCGTGGCCACTAC; 3, ATCGTGCTCTCCGAAGTGCGTTACTCGGGC; 4, GAGTTACTCGGACATGTCCACAAATG; 5, CGGAAAACCAGACGGATATTTT; 6, CATCTGTGCGACTTGGGT; 7, GTGCACTTCGTTCTCTTCAATCGTGCTGATCT; 10, AGGCCTTGGAAGTTCGGGACACTG; 11, CAGAAGGAATTCAGCTCGGGTCTGCC; 12, GCCATTCGACGAGACCTAAGGGGACACCAATTCCTTGC; 13, GCTGGGTCTTGGACAAGGCCATGGTGTCTTTGCGCTACTA; 14, CCGTTTTTAATATGGATATGCGGGCGATACTACGAGTAGC; 15, CAGCACAACTTCCTCAACTCCTACTACTTCTAC; 16, TGATGTTGGTGCATGAAGGAGCTCCGGTGAAC; 17, GGAACTCCGGTGCACCACGACTTCACAGGATGTGTTCTAC; 18, TCATTATTCACGCCATGTTTCGATGTGTGTGCTTCAATCG; 19, CTTCAATCGACATGGTCTGGCGCGACTAATGATC; 20, GAGCAACTAATGAGCATTACTCTAAAGGTGCAAATGCAATA; KATP1, GAGGAGATAGGCCAAGGCGTCAATGCCAA-GG; MATP1, CTCTCCGGAGAGAGTGGCGCGGGCAAGTCCA.

Protein Analyses

To check the NINAC protein levels in the different transformant lines, extracts were prepared as described from fly heads collected <2 d posteclosion after rearing under L/D conditions at 18°, 25° or 29°C (Mcntell and Rubin, 1988). The proteins were then fractionated on SDS–6% polyacrylamide gels, transferred to nitrocellulose, and probed with the rabbit antisera αZB551 diluted 1:1,000 (see Figs. 5 *A* and 7 *A*) or a cocktail containing both αp132 (1:1,500) and αp174 (1:4,000) (see Fig. 2) as previously described (Porter et al., 1992). The relative concentrations of p132 and p174 in the transformant lines were estimated by quantifying the radioactivity in protein blots using a PhosphorImage Analyzer (Molecular Dynamics, Every Cedex, France) and a storage phosphorscreen.

Electroretinogram Recordings

All ERG recordings were performed on flies in a $white^+$ (w^+)[1] background by applying glass electrodes, filled with Ringer's solution, to small drops of electrode cream (Sigma Immunochemicals, St. Louis, MO) placed on the surface of the compound eye and the thorax. The light source was a projector (model 765; Newport Corp., Irvine, CA) with a 100-W quartz tungsten–halogen lamp. The intensity of unfiltered light was ~20 mW/cm^2. The electroretinograms (ERGs) were amplified using a WPI Dam 60 differential amplifier and recorded on a Macintosh SE using a MacLab analog-digital converter and the Chart/4 v3.1 program. Because of limitations in the sampling rate of the MacLab analog-digital converter and the Chart/4 v3.1 program, the on-transients were frequently not detected even in wild-type flies. Therefore, it is not possible to reliably assess whether there is a defect in the on-transients in any of the transformant lines. All ERGs were performed on young flies (<2-d posteclosion) after immobilizing the flies in bee's wax. Before the first light pulse, the flies were dark-adapted for 60 s. The flies were exposed to pulses of light 4 s each, separated by an interval of 5 s. Transformant lines reared at 18° and 29°C were analyzed at the same temperature at which they were reared.

Analyses of Rhabdomeral Morphology

To determine the extent of retinal degeneration, flies (in a w^+ background) were reared under a 12 h light/12 h dark cycle for 3–4 wk at 25° or 29°C or 6–7 wk at 18°C. During the 12-h light periods, the flies were exposed to ~0.4 mW from a Phillips F40CW bulb. Samples of wild-type, $ninaC^{P235}$ and P[$ninaC^{KD}$] heads were prepared for examination by transmission EM by fixation in paraformaldehyde, glutaraldehyde, and sodium cacodylate, postfixation in osmium tetroxide, dehydration in an ethanol series, and embedding in Spurr's medium as described (Porter et al., 1992). 85-nm sections were examined by transmission EM.

All of the transformant lines were examined for retinal degeneration by performing the optical neutralization technique which facilitated the imaging of individual rhabdomeres within each ommatidium in whole mounts of adult heads (Franceschini and Kirschfeld, 1971). Briefly, fly heads were dissected and submerged in a small well of immersion oil and a coverslip was applied. The rhabdomeres were then examined at 600× using maximum intensity anadromic illumination on a Microphot FXA (Nikon, Garden City, NY) microscope with the condenser diaphragm closed to the minimum aperture opening.

Immunolocalization

The p174-specific antiserum (αp174) used for the immunolocalization was generated in rabbits to an *Escherichia coli* fusion protein consisting of the COOH-terminal end of the p174 tail joined to β-galactosidase as previously described (Porter et al., 1992). p174-specific antibodies were affinity purified from 0.3 ml of crude αp174 rabbit serum as previously described (Pollard, 1984). Briefly, the p174-specific antibodies were adsorbed onto nitrocellulose strips of p174 and the antibodies were eluted with acetic acid, neutralized, and dialyzed. The final volume of affinity purified αp174 was 1.5 ml.

Immunolocalization was performed on hemisected fly heads prepared from w^{1118};P[$ninaC^+$] (positive control), w^{1118};P[$ninaC^{MD}$], w^{1118};P[$ninaC^{KD}$], w^{1118};P[$ninaC^{366R}$], w^{1118};P[$ninaC^{968.2}$] and w^{1118}; $ninaC^{P235}$ (negative control) collected <24 h post-eclosion after being reared at 18°,

1. *Abbreviations used in this paper*: ERG, electroretinogram; L/D, light/dark; TEM, transmission EM; w^+, $white^+$.

25°, or 29°C under 12 h light/12 h dark conditions. The tissue was fixed in 3% paraformaldehyde, 3.5% sucrose, and 0.1 M phosphate (pH 7.4) for 3 h at 4°C, rinsed three times with 0.1 M phosphate (pH 7.4), and then dehydrated in an acetone series (50, 70, and 90%) for 30 min per incubation. The eyes were then infiltrated for ~20 h at 4°C with L.R. White (Polysciences Inc., Warrington, PA) and embedded in L.R. white for 24 h at 60°C. 0.5-μm sections were cut and placed on freshly gelatinized slides. The sections were blocked using 50 μl of 4% BSA, 1% goat serum in PBS for 30 min at room temperature, and then incubated overnight at 4°C with 50 μl of affinity-purified p174 diluted 1:10 in blocking solution. The sections were then washed with PBS, incubated 1 h with 50 μl of affinity-purified FITC-labeled goat anti-rabbit antiserum (Vector Laboratories Inc., Burlingame, CA) diluted 1:50 in blocking solution and washed with PBS. 15 μl of FITC-guard (Testog Inc., Chicago, IL) was then added and a coverslip was mounted. Confocal fluorescent images were obtained using an MRC 600 confocal imaging system (Bio-Rad Laboratories, Richmond, CA) on an Optiphot microscope and printed with a Mitsubishi CP210U color video copy processor. Immunolocalization studies were also performed on the same fly stocks listed above in a w^+ background using a secondary antibody conjugated to HRP.

Results

Construction of Transformant Lines with Mutated Kinase Domains

To test the roles of the *ninaC* kinase domain, we constructed two oligonucleotide-directed mutations which either deleted the entire protein kinase domain (amino acids 17 to 284) or changed a lysine, amino acid 45, to a methionine (Fig. 1). Amino acid 45 corresponds to the lysine shown to be the ATP-binding site in other protein kinases (Fry et al., 1986; Knighton et al., 1991). The altered *ninaC* genes and a wild-type control were introduced by P element-mediated germline transformation into a null allele, $ninaC^{P235}$, and multiple transformants were obtained. The transformants that contained the kinase deletion and lysine to methionine mutation at amino acid 45 were designated P[$ninaC^{KD}$] and P[$ninaC^{45M}$], respectively. These and other transformants containing mutations in *ninaC* (described below) will be referred to as alleles even though this designation typically refers to derivatives of the gene at the normal chromosomal position.

The requirements for the *ninaC* kinase domain in the photoreceptor cells were assessed by analyzing P[$ninaC^{KD}$] flies since the truncated form of p174 protein in P[$ninaC^{KD}$], 143 kD, was stable whereas both NINAC proteins were unstable in P[$ninaC^{45M}$]. The concentrations of the altered NINAC proteins were checked by probing an immunoblot containing protein extracts prepared from the two transformant lines. The levels of both p174 and p132 were reduced five- to tenfold in P[$ninaC^{45M}$] flies (Fig. 2). In P[$ninaC^{KD}$], although the deleted form of p174, 143 kD, was stable, the level of the truncated derivative of p132, 101 kD, was decreased fivefold. The concentration of the 143 kD protein in P[$ninaC^{KD}$] was intermediate between the p174 levels in homozygous wild-type and heterozygous wild-type $ninaC^{P235}$/+ flies. The instability of the 101-kD protein did not complicate the phenotypic analysis of P[$ninaC^{KD}$] flies since p132 is not required for a wild-type ERG or to prevent retinal degeneration (Porter et al., 1992).

The Protein Kinase Domain Is Required for a Normal ERG but Not to Prevent Retinal Degeneration

Analyses of P[$ninaC^{KD}$] flies demonstrated that the protein kinase domain was required for a normal ERG, but the

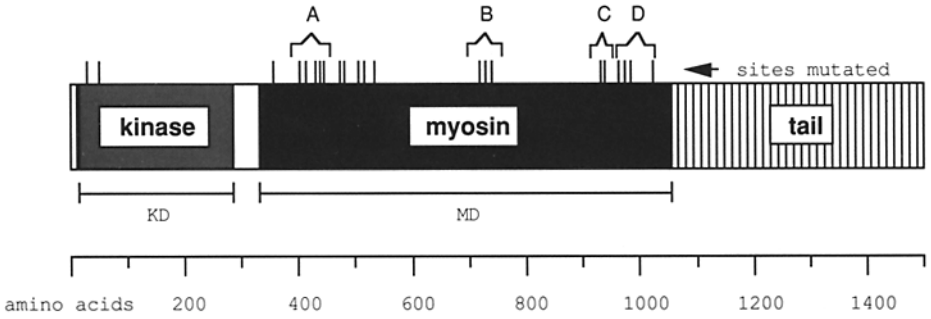

transformant	oligo	aa#	mutation	transformant	oligo	aa#	mutation
$ninaC^{KD}$	KD	17-284	deletion	$ninaC^{502.4}$	14	502-506	YXLEK→DXRAI
$ninaC^{23G}$	KATP1	23	A→G	$ninaC^{508C}$	2	508	R→C
$ninaC^{45M}$	KX	45	K→M	$ninaC^{520LNS}$	15	520-522	HIF→LNS
$ninaC^{MD}$	MD	331-1032	deletion	$ninaC^{707.4}$	18	707-712	DXXGFE→AXXRCV
$ninaC^{366R}$	1	366	G→R	$ninaC^{717.3}$	19	717-721	NXXEQ→HXXAR
$ninaC^{399TD}$	5	399-400	PH→TD	$ninaC^{724.4}$	20	724-729	INXXNE→SIXXKV
$ninaC^{409D}$	6	409	Y→D	$ninaC^{924\Delta3}$	9	924-926	NLG→---
$ninaC^{425EVR}$	3	425-427	GES→EVR	$ninaC^{931LFN}$	7	931-933	RCI→LFN
$ninaC^{428GA}$	MATP1	428-429	YS→GA	$ninaC^{957.2}$	10	957-959	GXL→EXR
$ninaC^{430DM}$	4	430-431	GK→DM	$ninaC^{968.2}$	11	968-972	GXXXR→EXXXG
$ninaC^{468.3}$	16	468-471	NAXT→HEXA	$ninaC^{978.3}$	12	978-982	FXXRY→DXXGH
$ninaC^{474.4}$	17	474-479	NNXSXR→HHXFXG	$ninaC^{1015.4}$	13	1015-1020	GXTKXF→DXAMXS

Figure 1. Oligonucleotide-directed mutations of *ninaC*. The block diagram represents p174. The positions of the site-directed mutations are indicated by the vertical lines above the diagram. The domains deleted by the $ninaC^{KD}$ and $ninaC^{MD}$ mutations are designated by the horizontal lines below the representation of p174. The letters above the diagram denote highly conserved myosin regions which were targeted for mutagenesis: (*A*) the putative ATP-binding site and flanking region; (*B*) a conserved region of unknown function; (*C*) the putative actin-binding site; and (*D*) a conserved region between the putative actin- and light-chain/calmodulin-binding domains. The table lists all the mutations constructed. Indicated in the table are the abbreviated names of the transformants (*transformant*), the designations of the mutating oligonucleotide-primers (*oligo*), the amino acids affected (*aa#*), and the actual alterations for each mutation (*mutation*). One letter abbreviations are used to indicate the amino acid changes and X indicates an unchanged amino acid.

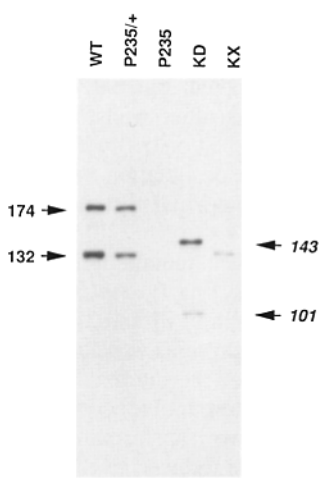

Figure 2. Protein blot showing expression of NINAC in kinase domain transformants. Protein extracts were prepared as described (Montell and Rubin, 1988) from the heads of the following flies <2-d post eclosion: wild-type homozygous transformant (*WT*), wild-type heterozygous transformant (P235/+), *ninaC*^{P235} null mutant (*P235*), P[*ninaC*^{KD}] (*KD*), and P[*ninaC*^{KX}] (*KX*). Extracts were fractionated on a SDS-6% polyacrylamide gel, transferred to nitrocellulose, probed with a primary *ninaC* antisera cocktail, αpl74 (1:4,000 dilution) and αpl32 (1:1,500 dilution) (Porter et al., 1992), and finally with ^{125}I-labeled protein A. Numbers indicate in kilodaltons the size of the wild-type and altered ninaC proteins. The sizes of the truncated NINAC proteins expressed in P[*ninaC*^{KD}] are indicated to the right in italics.

P[*ninaC*^{KD}] phenotype was distinct from the null allele, *ninaC*^{P235}. Shown in Fig. 3 are the ERG responses to two pulses of light obtained with wild-type, *ninaC*^{P235} and P[*ninaC*^{KD}] flies after a 60 s dark-adaptation. ERGs assay the response of all cells in the retina to light. Wild-type flies displayed a corneal negative response to light which was maintained for the duration of the light pulse with little diminution (Fig. 3 *A*). Upon cessation of the light stimulus, the maintained component of the ERG rapidly returned to the dark state. Coincident with the initiation and termination of the light stimuli, were transient positive and negative potentials, referred to as on and off transients. These transient spikes derive from activity post-synaptic to the photoreceptor cells in the luminal portion of the optic lobe (Buchner, 1991). The ERG response to the second pulse of light, with wild-type flies, is similar to the first.

The ERG obtained with *ninaC*^{P235} is characterized by a larger corneal negative receptor potential in response to the first pulse than to the second (Porter et al., 1992; Fig. 3 *B*). The amplitude of the first corneal negative response is typically larger than that of wild-type flies. Upon, cessation of the first light stimulus, the return to the dark state is slower in *ninaC*^{P235}. In addition, the amplitude of the off transient is usually markedly reduced. The response of *ninaC*^{P235} flies to a second light stimulus is less defective. The amplitude of the second corneal negative ERG is typically similar in amplitude to wild-type. However, the off transient is still reduced and the rate of return to the dark state is slightly retarded.

The ERG response obtained with P[*ninaC*^{KD}] flies was defective, but distinct from the ERG elicited with *ninaC*^{P235} (Fig. 3 *C*). Both *ninaC*^{P235} and P[*ninaC*^{KD}] were characterized by a large corneal negative response to the first pulse of light. However, the decline of the maintained component during the first light stimulus was more pronounced in P[*ninaC*^{KD}] than *ninaC*^{P235}. Two other features of the P[*ninaC*^{KD}] ERG differed from the null allele. The decline in the corneal negative potential after cessation of the light stimulus was less dramatic in P[*ninaC*^{KD}] and no defect in the offtransients was observed. In contrast to *ninaC*^{P235} flies, the response of P[*ninaC*^{KD}] flies to a second light stimulus was indistinguishable from wild type. Thus, it appeared that P[*ninaC*^{KD}] flies were characterized by a ERG phenotype that displayed some but not all of the features typical of a *ninaC*^{P235} ERG. P[*ninaC*^{45M}] flies, which expressed five- to tenfold less NINAC than wild-type flies, displayed an ERG phenotype indistinguishable from *ninaC*^{P235}. This null phenotype was most likely due to the instability of pl74 in P[*ninaC*^{45M}] flies.

In contrast to *ninaC*^{P235}, P[*ninaC*^{KD}] flies did not undergo retinal degeneration. Retinal degeneration was assessed following aging of flies for 21 d on a 12-h light/12 h dark cycle

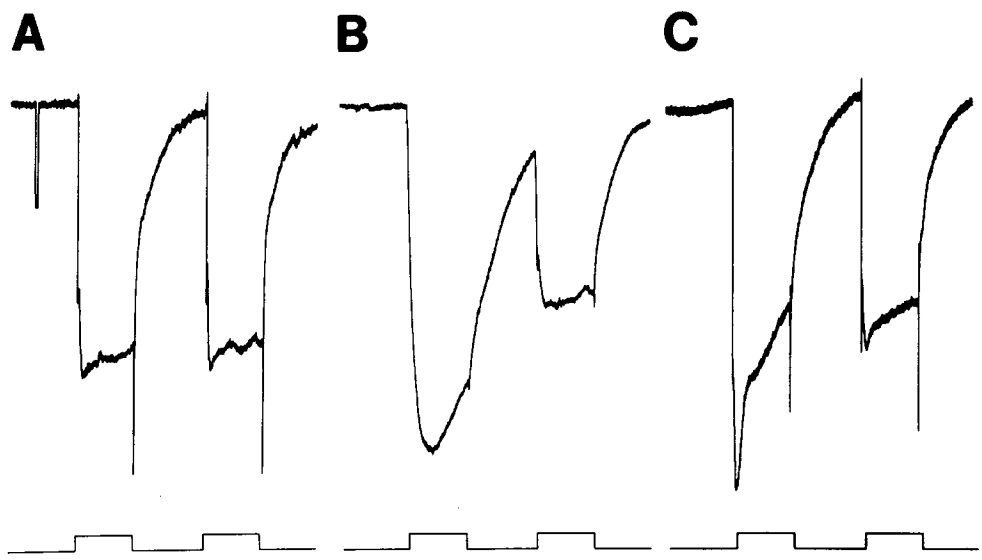

Figure 3. Electroretinogram phenotype of the kinase deletion mutant, P[*ninaC*^{KD}]. ERGs were performed on flies reared under a 12 h light/12 h dark cycle and collected <2-d post-eclosion. After immobilizing the flies for the ERGs in dim light, they were dark adapted for 60 s before initiation of the ERG. The initiation and cessation of the 4-s light response is indicated by the event marker below the ERGs. The interval between the two light pulses was 5 s. The transient response 3 s before the initiation of the first light stimulus in *A* is a 5 mV calibration pulse. (*A*) Wild-type transformant (P[*ninaC*$^{+}$]); (*B*) null mutant (*ninaC*^{P235}); (*C*) kinase deletion mutant (P[*ninaC*^{KD}]).

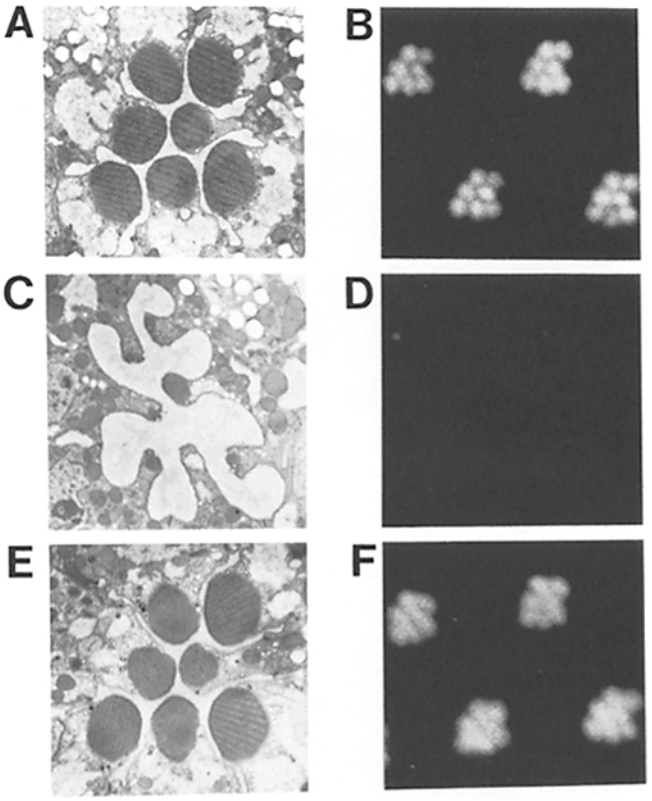

Figure 4. Morphology of wild-type (P[*ninaC*$^{+}$]), *ninaC*^{P235}, and P[*ninaC*^{KD}] flies observed by transmission EM and the optical neutralization technique. *A*, *C*, and *E* are tangential sections of compound eyes, from 21-d-old flies reared on 12 h light/12 dark cycle, viewed by transmission EM. A single ommatidium at a depth of 30 μm is shown. The seven rhabdomeres corresponding to the six outer photoreceptor cells, R1-6, and the central photoreceptor cell, R7, are the seven large oval structures arranged in a trapezoidal pattern. *B*, *D*, and *F* are light microscopic images of rhabdomeres visualized by the optical neutralization technique. Each panel shows the rhabdomeres from four ommatidia. (*A* and *B*) Wild-type transformants P[*ninaC*$^{+}$]; (*C* and *D*) null mutant (*ninaC*^{P235}); (*E* and *F*) kinase deletion mutant P[*ninaC*^{KD}].

(L/D) by examining the ultrastructure of the rhabdomeres using transmission EM (TEM). The diameter of the rhabdomeres in wild-type flies does not change with age or with exposure to light (Porter et al., 1992; Fig. 4 *A*). This was in contrast to *ninaC*^{P235}, in which the rhabdomeres gradually degenerate during a 21-d L/D cycle (Porter et al., 1992; Fig. 4 *C*). Most of the retinal degeneration can be prevented by maintaining the flies in the dark (Porter et al., 1992). We found that in P[*ninaC*^{KD}] flies, no retinal degeneration was detected (Fig. 4 *E*). The morphology of the wild type, *ninaC*^{P235}, and P[*ninaC*^{KD}] is also shown by the optical neutralization technique for comparison with the TEM since this is the technique used to analyze the rest of the mutants described below. The optical neutralization technique is a rapid method that facilitates imaging individual rhabdomeres within each ommatidium in whole mounts of adult heads (see Materials and Methods, Franceschini and Kirschfeld, 1971). However, subtle alterations in morphology would not be detected using this method. Of primary significance here, the results demonstrated that the kinase domain did not function to maintain the rhabdomeres. Furthermore, the ERG and retinal degeneration phenotypes were not obligatorily coupled, it was possible to obtain a *ninaC* mutation that caused an ERG phenotype without inducing retinal degeneration (Table I).

The Myosin Head Domain Is Required for a Wild-type ERG and to Prevent Degeneration

To address the role of the myosin domain, the entire domain was deleted from the wild-type gene (amino acids 331–1032) which was then introduced into the null allele, *ninaC*^{P235}, by germline transformation and several transformants lines, referred to as P[*ninaC*^{MD}], were obtained (Fig. 1). The concentrations of NINAC expressed in each of the transformant lines was determined by performing an immunoblot (Fig. 5 *A*). A single representative line is shown since little variability in protein levels was observed among the transformants. The truncated form of p174, 93 kD, was detected at wild-type levels in P[*ninaC*^{MD}] flies, however, the concentration of the 50-kD derivative of p132 was greatly reduced (Fig. 5 *A*).

Table I. Phenotype Summary of Selected Transformant Lines

Fly stock	Mutation	Temperature	ERG	Morphology	p174 protein level	p174 localization
Wild-type	None	18°C, 25°C, 29°C	+	+	+	Rhabdomere
ninaC^{P235}	Null	18°C, 25°C, 29°C	−	−	−	None
P[*ninaC*^{KD}]	Kinase deletion	18°C, 25°C, 29°C	∓	+	+	Rhabdomere
P[*ninaC*^{MD}]	Myosin deletion	18°C, 25°C, 29°C	−	−	+	Rhabdomere and cell body
P[*ninaC*^{366R}] and P[*ninaC*$^{968.2}$]	(ts) Myosin point mutants	18°C	+	+	+	Rhabdomere
		29°C	+	−	+	Rhabdomere and cell body

The ERG and morphological phenotypes of the most informative alleles in this study are listed along with the nature of the mutation, the temperatures at which the analyses were performed, the NINAC p174 protein levels and spatial localizations of p174. Results for wild-type and *ninaP*^{235} null mutant flies are included. For ERG and morphological analyses: (+) normal or wild-type results; (−) a defective or mutant phenotype; and (∓) a partially defective ERG. For protein levels (+) indicates at least 50% of wild-type levels. Protein levels and p174 spatial localizations were not examined at 18° or 29°C for P[*ninaC*^{KD}] or P[*ninaC*^{MD}].

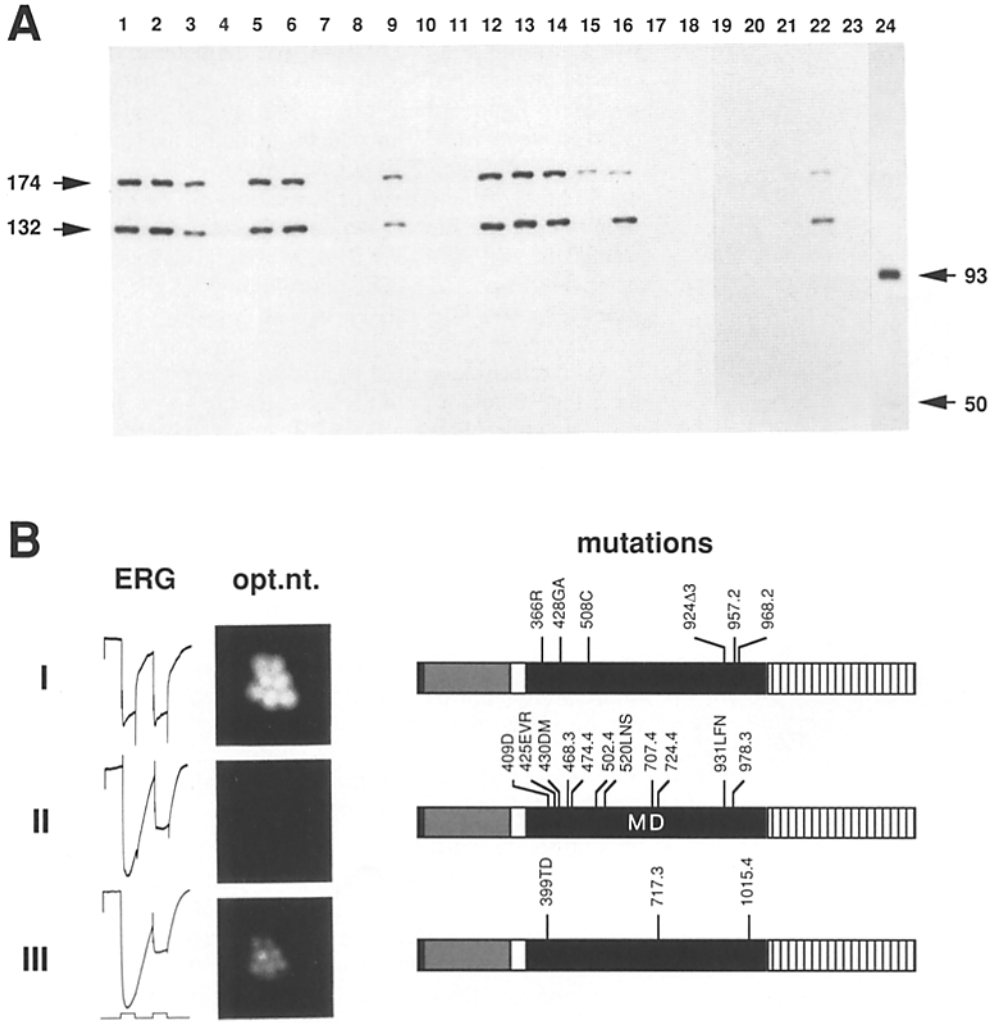

Figure 5. Protein blot and phenotypic analyses of myosin domain mutants reared at 25°C. (*A*) Western blot of myosin mutant head extracts fractionated on a SDS-polyacrylamide gel, transferred to nitrocellulose, and probed with the *ninaC* specific antisera, αZB551 (Montell and Rubin, 1988), which reacts to both isoforms. The sizes of the NINAC proteins in the point mutants and in the deletion mutant, P[$ninaC^{MD}$], are indicated to the left (132 and 174) and right (50 and 93) in kilodaltons. Lanes were loaded as follows: (*1*) wild-type Canton S; (*2*) wild-type homozygote transformant (P[$ninaC^{+}$]/P[$ninaC^{+}$]); (*3*) wild-type heterozygote [P[$ninaC^{+}$]/$ninaC^{P235}$); (*4*) null mutant ($ninaC^{P235}$); (*5*) P[$ninaC^{366R}$]; (*6*) P[$ninaC^{508C}$]; (*7*) P[$ninaC^{425EVR}$]; (*8*) P[$ninaC^{430DM}$]; (*9*) P[$ninaC^{399TD}$]; (10) P[$ninaC^{409D}$]; (*11*) P[$ninaC^{931LFN}$]; (*12*) P[$ninaC^{924\Delta 3}$]; (*13*) P[$ninaC^{957.2}$]; (*14*) P[$ninaC^{968.2}$]; (*15*) P[$ninaC^{978.3}$]; (*16*) P[$ninaC^{1015.4}$]; (*17*) P[$ninaC^{502.4}$]; (*18*) P[$ninaC^{520LNS}$]; (*19*) P[$ninaC^{468.3}$]; (20) P[$ninaC^{474.4}$]; (*21*) P[$ninaC^{707.4}$]; (22) P[$ninaC^{717.3}$]; (*23*) P[$ninaC^{724.4}$]; and (*24*) P[$ninaC^{MD}$]. All extracts were from flies collected <2-d post-eclosion after rearing under L/D conditions. All transformant flies were homozygous for the P element insert. (*B*) Electrophysiological and morphological characteristics of the myosin mutants. Mutants fell into three phenotypic classes: (*I*) wild-type; (*II*) null phenotype; (*III*) null ERG phenotype and intermediate level of retinal degeneration. All ERGs were performed on flies <2-d post-eclosion. The paradigm for the ERGs was the same as in Fig. 3. The initiation and cessation of the 4-s light response is indicated by the event marker below the ERGs. The interval between the two light pulses was 5 s. The transient response 3 s before the initiation of the first light stimulus was a 5 mV calibration pulse. The optical neutralization technique was performed on flies maintained for 3–4 wk under a L/D cycle. Shown are the ERG recordings and rhabdomeres from a single ommatidium from representative group I (P[$ninaC^{508C}$]), group II (P[$ninaC^{MD}$]), and group III (P[$ninaC^{717.3}$]) flies. The positions of the mutations that resulted in group I, II, or III phenotypes is indicated to the right.

Since only p174 is required for a wild-type ERG and to prevent retinal degeneration (Porter et al., 1992), the instability of the truncated version of p132 did not complicate the phenotypic analyses of P[$ninaC^{MD}$].

P[$ninaC^{MD}$] flies were examined for defects in phototransduction, on the basis of ERGs, and for retinal degeneration, using the optical neutralization technique. We found that P[$ninaC^{MD}$] flies were characterized by a phenotype indistinguishable from the null allele (Table I). The P[$ninaC^{MD}$] ERG exhibited all the features typical of a $ninaC^{P235}$ ERG, a large corneal negative response, decreased transients, and slow return of the maintained component to the dark state after cessation of the first light stimulus (Fig. 5 *B*). P[$ninaC^{MD}$] flies maintained for 21 d under a L/D cycle also showed as severe degeneration of the rhabdomeres as $ninaC^{P235}$ (Fig. 5 *B*). These results suggest that the myosin domain was required for normal phototransduction and to prevent retinal degeneration; however, they do not resolve

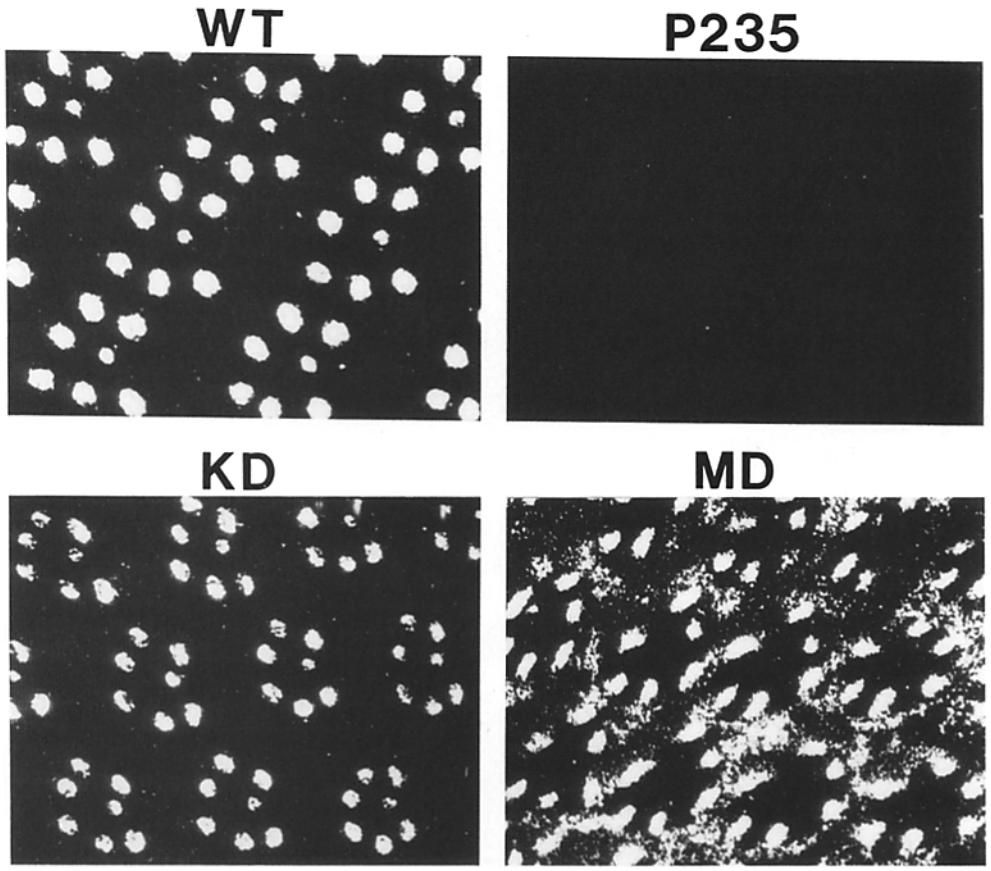

Figure 6. Immunolocalization of p174 in the kinase and myosin deletion mutants. Tangential 0.5-μm sections, at a depth of 30 μm, prepared from fly heads embedded in L. R. White were probed with αp174 followed by a fluorescein-labeled secondary antibody. (WT) Wild-type transformant (w^{1118}; P[$ninaC^{+}$]); null mutant (w^{1118}; $ninaC^{P235}$); (*KD*) kinase deletion mutant (w^{1118};P[$ninaC^{KD}$]); (*MD*) myosin deletion mutant (w^{1118}; P[$ninaC^{MD}$]). All flies were reared at 25°C under normal L/D conditions and collected <1-d posteclosion. Immunolocalization studies were also performed on the same fly stocks listed above in a w^{+} background using a secondary antibody conjugated to HRP and results indistinguishable from those shown here were obtained (data not shown).

the issue as to whether the retinal degeneration was a secondary effect of the ERG phenotype.

The Myosin Head Domain Is Required to Concentrate p174 in the Rhabdomeres

We have shown that the COOH-terminal tail unique to p174 is required for localization to the rhabdomeres (Porter et al., 1992). To determine whether the myosin or kinase domains were also required for rhabdomeral localization, we examined the subcellular localization of the truncated p174 proteins, in P[$ninaC^{MD}$] and P[$ninaC^{KD}$]. We stained sections of wild-type and mutant compound eyes with an antiserum, αp174, which specifically reacts with the p174-unique tail. The p174 protein was localized specifically to the rhabdomeres in wild-type flies and no p174 staining was detected in $ninaC^{P235}$ (Fig. 6). The staining pattern in P[$ninaC^{KD}$] was also rhabdomere specific. However, in P[$ninaC^{MD}$] photoreceptor cells, p174 was not localized exclusively to the rhabdomeres, but was detected in the cell body as well (Fig. 6, Table I). The distribution in both the rhabdomeres and cell body was not an artifact associated with rhabdomere degeneration since the sections were prepared from young *ninaC* flies which had not undergone any significant retinal degeneration. Furthermore, degeneration of the rhabdomeres in another retinal degeneration mutant, *rdg*A, does not cause p174 to become localized to the cell body; rather p174 degrades along with the rhabdomeres and is not detected (Hicks and Williams, 1992).

Phenotypes of Point Mutations in the Myosin Domain at 25°C

A series of mutations was constructed in which one to four amino acids conserved among most known myosins were changed (Fig. 1). Each of the mutant *ninaC* genes was introduced into the null allele, $ninaC^{P235}$, by germline transformation and multiple transformants lines were established for each. Although many of these mutations altered more than one amino acid, they will be referred to as point mutations to distinguish them from the mutations that deleted the entire kinase or myosin domain. Most of the point mutations were expected to disrupt *ninaC* function since they were in residues conserved in *ninaC* and most known myosins. Therefore, to support the contention that the mutations in conserved residues disrupted function because the amino acids were critical and not because most any random mutation in *ninaC* would disrupt function, we constructed three additional mutations that altered *ninaC* so that the sequence would better conform to known myosins and protein kinases (see below).

The concentration of NINAC expressed in each line was determined by performing an immunoblot (Fig. 5 *A*). Although the myosin-deleted form of p174, p93, was present at wild-type levels in P[$ninaC^{MD}$], in 14 of the 18 mutants in which conserved residues in the myosin domain were changed, the concentrations of both NINAC proteins were decreased. In contrast, both mutations in the myosin domain that altered the *ninaC* sequence so as to conform better to known myo-

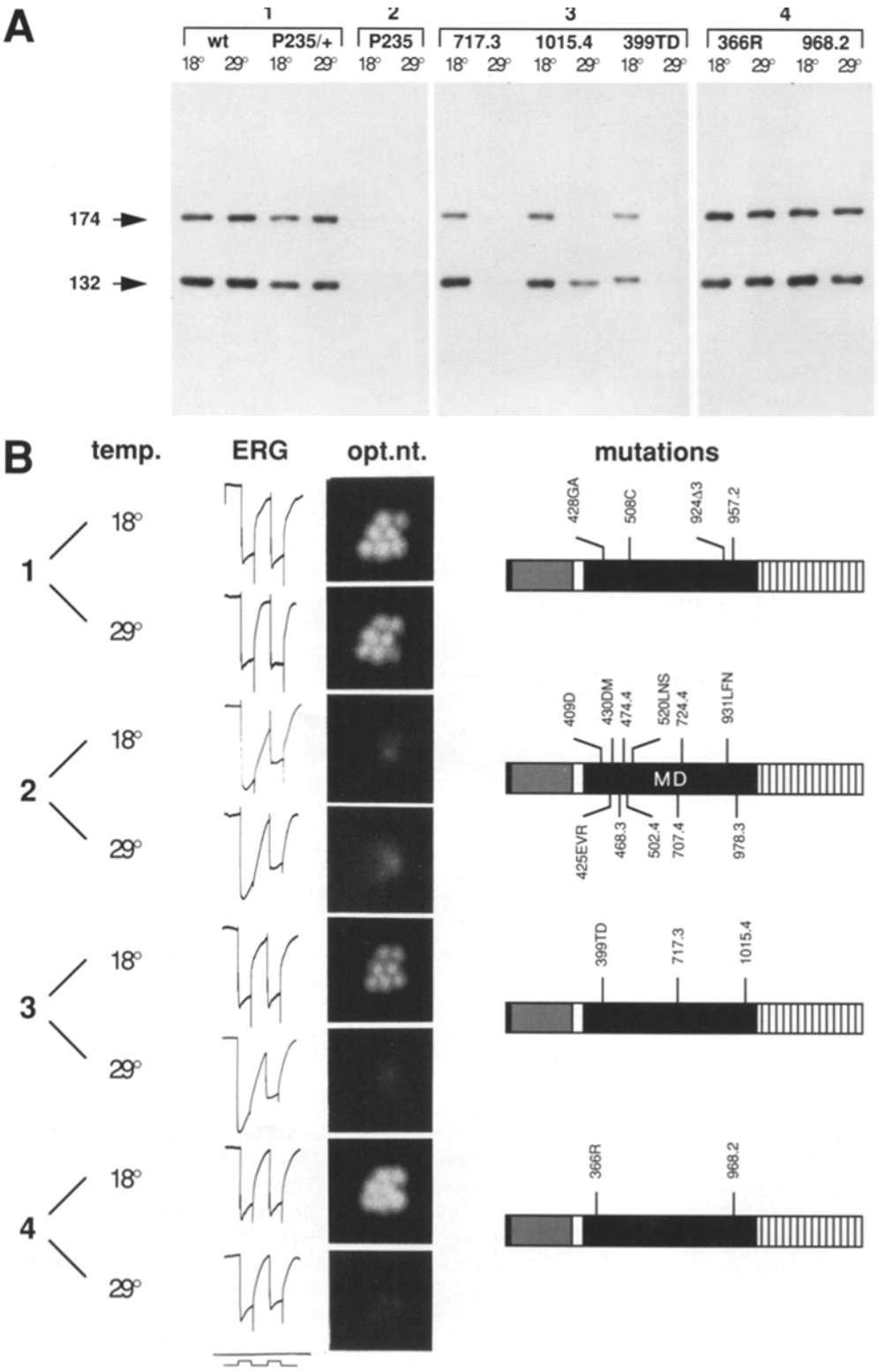

Figure 7. Temperature-dependent phenotypes of myosin domain mutants. (*A*) Western blot of head extracts prepared from myosin domain transformant lines that showed phenotypic differences at 18 and 29°C. Lanes were loaded with extracts from the indicated transformant lines reared at 18° and 29°C and collected <2-d posteclosion. The numbers are above the brackets in *A* and to the left in *B* indicate the four phenotypic classes which emerged from the temperature analyses (see text). (*B*) ERG and rhabdomere morphology of the myosin mutants reared at 18° and 29°C. ERGs were performed on flies <2-d posteclosion reared at the indicated temperature. The initiation and cessation of the 4-s light response is indicated by the event marker below the ERGs. The interval between the two light pulses was 5 s. The transient response 3 s before the initiation of the first light stimulus in the group 1 18°C ERG was a 5 mV calibration pulse. Rhabdomere morphology was assessed by performing the optical neutralization technique on flies reared at 29°C, and aged for 3–4 wk under a 12 h light/12 h dark cycle, or at 18°C, after aging for 6–7 wk under 12 h light/12 h dark cycle. The transformants which fell into each of the four classes is indicated to the right.

sins, ninaC^{428A} and ninaC$^{924\Delta3}$, resulted in expression of wild-type concentrations of NINAC (e.g., see Fig. 5 for P[*ninaC*$^{924\Delta3}$]) as did the mutation (P[*ninaC*^{KAP1}]) that improved the kinase homology.

The transformants were initially characterized at 25°C and subsequently at 18° and 29°C to determine whether any exhibited temperature-sensitive phenotypes (see below). Based on phenotypic analyses at 25°C, the transformants fell into three classes (Fig. 5).

Group I transformants were wild type. These consisted of six transformants which accumulated both NINAC proteins at wild-type levels (Fig. 5, *A* and *B*). Among these six were two, P[*ninaC*^{366R}] and P[*ninaC*^{508C}], that changed the corresponding glycine and arginine residues in *ninaC* altered in

the *Caenorhabditus elegans unc-54* muscle myosin alleles, s95 and s74, respectively (Dibb et al., 1985). These mutations changed conserved amino acids flanking the putative ATP-binding site (reviewed in Warrick and Spudich, 1987). In *C. elegans*, neither s95 nor s74 interferes with myosin assembly or results in paralysis; however, both mutations cause the animals to move very slowly. Therefore, the ninaC^{366R} and ninaC^{508C} mutations were particularly good candidates for mutations that might result in weak phenotypes. Two other group I transformants, P[*ninaC*^{428GA}] and P[*ninaC*$^{924\Delta 3}$] (Fig. 1), were expected to be wild-type since, unlike all the other myosin mutations, they changed the *ninaC* sequence so as to conform better to the myosin consensus.

The largest phenotypic class, group II, which included the myosin deletion mutant, P[*ninaC*^{MD}], described above, was characterized by a phenotype indistinguishable from the null allele. 11 point mutants also displayed null phenotypes (Fig. 5 *B*). The concentration of p174 was dramatically reduced in most but not all of the group II transformants. The most notable exception was P[*ninaC*^{MD}] in which the truncated p174 was detected at a level similar to wild type (see above). The concentration of p174 expressed in P[*ninaC*$^{978.3}$] was intermediate between P[*ninaC*^{MD}] and all the other group II point mutants (Fig. 5 *A*).

A third group of transformants (group III) was characterized by a null ERG phenotype and retinal degeneration less severe than the null mutants. One of these group III transformants, P[*ninaC*^{399TD}], expressed levels of p174 comparable to functionally wild-type heterozygotes (Fig. 5 *A*, Table I). Thus, it was possible for a point mutation in the myosin domain to cause a null ERG phenotype without causing a dramatic decrease in NINAC protein concentration. None of the phenotypes associated with any group II or III transformant was dominant (data not shown).

Identification of Two Alleles Displaying Temperature Dependent Retinal Degeneration

To determine whether any of the myosin domain mutations caused a temperature sensitive (ts) phenotype, each of the transformant lines was reared at 18° and 29°C and assayed for retinal degeneration and for defects in the ERG. Based on the phenotypes, the 21 transformants with mutations in the myosin domain were grouped into four classes. As was observed in the analysis of the transformants reared at 25°C, none of the transformants reared and analyzed at 18° and 29°C exhibited a dominant phenotype (data not shown).

The first class (group 1) consisted of transformants which were wild type at both temperatures and expressed NINAC at normal levels (Fig. 7). Four of the six transformants that were wild-type at 25°C were also wild-type at both 18° and 29°C. Among these group 1 transformants were P[*ninaC*^{428GA}] and P[*ninaC*$^{924\Delta 3}$] which were predicted to be wild type since they changed the myosin domain sequence so as to conform better to known myosins. Although both *ninaC* transformants, P[*ninaC*^{366R}] and P[*ninaC*^{508C}], corresponding to the weak *unc-54* alleles were wild type at 25°C, only P[*ninaC*^{508C}] was wild type at both 18° and 29°C. P[*ninaC*^{366R}] fell into a different class and is described below.

The second class (group 2) included lines which were mutant at 18° and 29°C (Fig. 7 *B*). All 12 alleles which exhibited null phenotypes at 25°C (Fig. 5), such as P[*ninaC*^{MD}], were similarly defective at 18° and 29°C. Most of the group 2 transformants expressed very low levels (<5%) of NINAC at both temperatures.

Five alleles were ts and comprised two different phenotypic classes (groups 3 and 4). Three of these lines (group 3), displayed a wild-type ERG and minor retinal degeneration at 18°C, but at 29°C exhibited a mutant ERG and severe retinal degeneration (Fig. 7, *A* and *B*). All three of these group 3 alleles fell into the same phenotypic class at 25°C as well (see Fig. 5, group 3), characterized by a defective ERG and moderate retinal degeneration. The phenotypes of the group 3 alleles, at 18° and 29°C, were paralleled by changes in stability of p174. At 18°C there was a slight, twofold decrease in p174 concentration, relative to the levels in wild-type flies, while at 29°C the concentration of p174 was dramatically reduced (<5%; Fig. 7 *A*).

The remaining two ts transformants (group 4) were characterized by severe retinal degeration, but a wild-type ERG, at the non-permissive temperature (Fig. 7 *B*; Table I). The group 4 transformants included P[*ninaC*$^{968.2}$], which contained a mutation near the COOH terminus of the myosin domain, and P[*ninaC*^{366R}] which had the corresponding point mutation identified in the weak *unc-54* allele, s95. P[*ninaC*^{366R}] was a particularly good candidate for a ts phenotype since it was predicted to reduce rather than eliminate the putative myosin activity in *ninaC*. The concentrations of NINAC, in both group 4 ts alleles, were wild type at 18° and 29°C (Fig. 7 *A*). At 18°C, neither P[*ninaC*^{366R}] nor P[*ninaC*$^{968.2}$] showed any discernible retinal degeneration and the ERGs were wild type. This was in contrast to the phenotype at 29°C, which was characterized by severe retinal degeneration; yet, the ERG waveform was wild type. The analysis of these ts alleles demonstrated that it is possible to obtain *ninaC* mutants that display retinal degeneration phenotype without affecting the ERG waveform (Table I).

Mislocalization of p174 in Temperature-sensitive Mutants at 29°C

To determine the subcellular localization of p174 in P[*ninaC*^{366R}] and P[*ninaC*$^{968.2}$] at 18° and 29°C, we performed immunolocalization. Sections were prepared from young adult flies, reared at 29°C, which had not undergone any significant retinal degeneration. We found that in wild-type flies, p174 was spatially restricted to the rhabdomeres at both 18° and 29°C (Fig. 8). The p174 protein was also localized exclusively to the rhabdomeres in P[*ninaC*^{366R}] flies reared at 18°C (Fig. 8). However, at 29°C, we found that p174 was distributed throughout the photoreceptor cells, in both the rhabdomeres and cell bodies (Fig. 8). Thus, a single amino acid substitution in the myosin domain was sufficient to alter the concentration of NINAC in the rhabdomeres and cell bodies. Localization of p174 in P[*ninaC*$^{968.2}$] was also restricted to the rhabdomeres at 18°C, and in both the cell bodies and rhabdomeres at 29°C (data not shown).

Discussion

The NINAC proteins are unique molecules consisting of a protein kinase domain joined to the head region of the myosin heavy chain. The unusual combination of these two domains raises the question as to the role of linkage of a protein kinase and a myosin domain. We have shown recently that

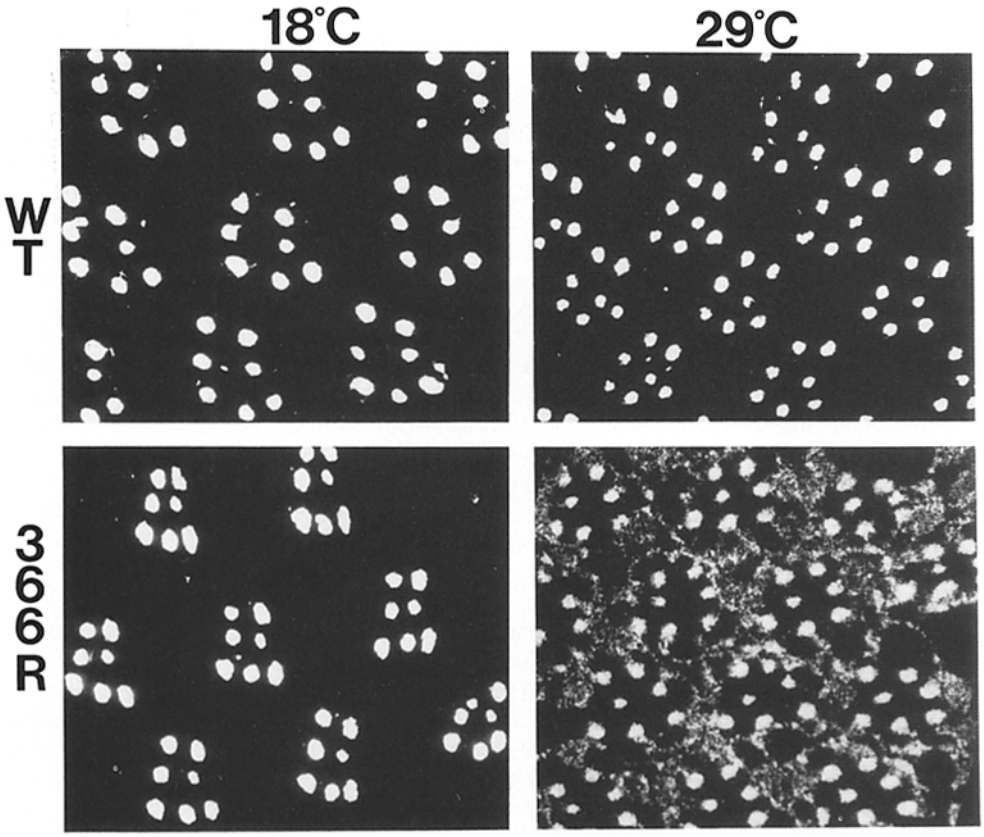

Figure 8. Immunolocalization of p174 in the temperature-sensitive transformant P[*ninaC*^{366R}]. Tangential 0.5-μm sections of adult wild-type (WT) and P[*ninaC*^{366R}] (366R) compound eyes were embedded in L. R. White, probed with αp174 and a fluorescein-labeled secondary antibody. Flies were reared at either 18° or 29°C under 12 h light/12 h dark conditions and collected <1-d post-eclosion. Immunolocalization studies were also performed on the same fly stocks listed above, at both 18° and 29°C, in a w^+ background using a secondary antibody conjugated to HRP and results indistinguishable from those shown here were obtained (data not shown).

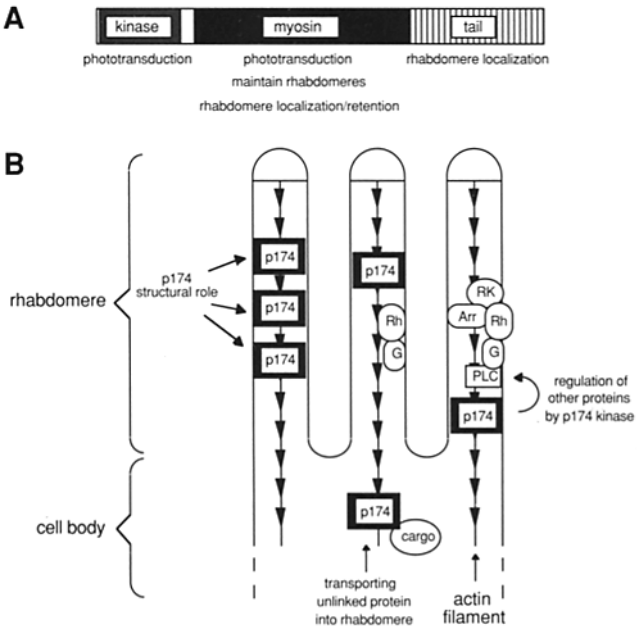

Figure 9. Functional domains and model for NINAC p174. (*A*) Functions of each domain, suggested by the phenotypes of the mutant transformants, are indicated below each domain. (*B*) Model of p174 function in the photoreceptor cells. Cartoon of a portion of a photoreceptor cell with p174 associated with actin filaments and membrane in the rhabdomere. The model suggests that the p174 kinase domain regulates other proteins required for phototransduction and the myosin domain serves multiple functions: to provide structural support necessary for maintaining the rhabdomeres and to provide actin-based access into the rhabdomeres for the linked p174 kinase and unliked cargo. Other rhabdomeric proteins involved in phototransduction are depicted as follows: rhodopsin (*Rh*), arrestin (*Arr*), rhodopsin kinase (*RK*), G-protein (*G*), phospholipase C (*PLC*), and putative p174 cargo (*cargo*).

p174 is a rhabdomere-specific protein required for normal phototransduction and to prevent light- and age-dependent retinal degeneration (Porter et al., 1992). Based on the ERG phenotype and the observation that *ninaC* encodes a putative protein kinase domain, one potential role for p174 is to regulate the activity of other proteins important in phototransduction by phosphorylation (Fig. 9 *B*). The myosin domain may be required to retain or traffic the kinase domain along the actin filaments in the rhabdomeres (Fig. 9 *B*). This could provide a mechanism for the kinase domain to access its rhabdomeric target(s). In addition, the myosin and tail domains may facilitate movement or retention in the rhabdomeres of one or more unlinked proteins required in phototransduction (Fig. 9 *B*).

To test the roles of the *ninaC* kinase and myosin domain individually, we constructed site-directed mutations that altered or deleted conserved amino acids or domains and assessed the phenotypic consequences of these mutations in the compound eye. The model for *ninaC* function described above would predict that both the kinase and myosin domains would be required for a normal ERG. If the myosin and tail domains function primarily to transport the kinase domain into the rhabdomeres, then mutation of the kinase domain should result in a null ERG phenotype. Alternatively, if the

myosin and tail domains also function to transport unlinked proteins important in phototransduction, then disruption of the kinase domain should result in a partial ERG phenotype and mutation of the myosin domain should elicit a null ERG phenotype. We have shown that *ninaC* flies display a mutant ERG before any discernible retinal degeneration suggesting that the altered ERG is not a secondary effect of the retinal degeneration (Porter et al., 1992). However, retinal degeneration could be a secondary effect of the phototransduction defect. If so, then the ERG and retinal degeneration phenotypes would be coupled and it would not be possible to generate mutations that elicit just one phenotype or the other. However, if the ERG and retinal degeneration phenotypes are not coupled, then it should be possible to cause one phenotype without the other. This would suggest that NINAC is required not only in phototransduction, but in addition plays a separate, structural role.

The Protein Kinase Domain Appears to Be Important in Phototransduction

We found that deletion of the kinase domain resulted in a partial ERG phenotype, but no retinal degeneration (Fig. 9 *A*, Table I). These results demonstrated that the electrophysiological and retinal degeneration phenotypes were not obligatorily coupled and suggest that p174 may have more than one role (see below). The observation that the kinase domain was required only for normal electrophysiology provided the strongest evidence to date that p174 has a specific role in phototransduction. The role of the putative kinase may be to regulate the activities of other rhabdomeric proteins important in phototransduction by phosphorylation. NINAC is most likely a serine/threonine kinase based on comparison of the deduced amino acid sequence to known protein kinases (Montell and Rubin, 1988). A number of proteins in the photoreceptor cells, including rhodopsin and arrestin, have been shown to undergo light-dependent serine/threonine phosphorylation (Matsumoto et al., 1984). The rhabdomere-specific p174 may play a role in regulating the activity of such rhabdomeric proteins important in phototransduction by serine/threonine phosphorylation.

The Myosin Domain Appears to Be Required to Traffic and/or Retain the Kinase Domain in the Rhabdomeres

One potential role for the myosin domain in p174 is to facilitate trafficking or retention of the kinase domain in the rhabdomeres (Fig. 9 *B*). We have shown previously that only p174, and not p132, is localized to the rhabdomeres indicating that the tail domain unique to p174 is required for rhabdomere localization (Porter et al., 1992). This previous study did not consider whether the myosin domain might also have a role in rhabdomere localization. In the current report, we showed that deletion of the myosin domain resulted in distribution of the altered version of p174 in both the cell bodies and rhabdomeres. This result suggests that the myosin domain plays a role, in addition to the tail, in the trafficking and/or retention of p174 in the rhabdomeres (Fig. 9 *A*).

The p174 myosin and tail domains may facilitate rhabdomere localization via different mechanisms. The tail of the Acanthamoeba myosin IC has been shown to bind to phospholipids (Doberstein and Pollard, 1992). Since the p174 and myosin IC tails share several common features, most notably a basic domain of several hundred amino acids, p174 may also bind phospholipids via its tail domain (Pollard et al., 1991). Turnover of the rhabdomeral membrane involves membrane shedding and insertion of new membrane at the base of the microvilli (reviewed in Blest, 1988). Binding of the p174 tail to phospholipid vesicles destined for the rhabdomere could provide a mechanism for p174 to be delivered to the rhabdomeres. Once in the rhabdomeres, p174 might bind to the actin filaments in the microvilli via the myosin domain. According to this model, deletion of the myosin domain might not affect the initial localization to the rhabdomeres but would prevent its retention since the truncated p174 derivative would presumably be unable to bind actin. Consistent with this model are the observations that p132, which is lacking the p174 tail, is completely in the cell body, whereas the altered form of p174 in P[$ninaC^{MD}$] is found in both the rhabdomeres and cell bodies.

p174 May Be Required to Transport Unlinked Proteins Important in Phototransduction into the Rhabdomeres

Deletion of the myosin domain resulted in a more severe ERG phenotype than deletion of the kinase domain. This suggests that the myosin may play a role in phototransduction in addition to trafficking the kinase domain into the rhabdomere. Since mechanical forces, by a putative motor molecule, have been shown to control the opening and closing of Ca^{2+} channels in hair cells, it is possible that the NINAC myosin domain also interacts with a channel protein in the rhabdomeres (Hudspeth, 1989; Assad and Corey, 1992). Alternatively, the myosin domain might function to transport or retain, in addition to the linked kinase domain, one or more unlinked proteins important in phototransduction into the rhabdomeres. Consistent with the proposal that p174 may facilitate rhabdomeral localization of an unlinked protein(s), we have found that calmodulin, which is normally localized predominantly in the rhabdomeres, is not concentrated in the rhabdomeres of flies lacking p174 (Porter, J. A., M. Yu, S. K. Doberstein, T. D. Pollard, and C. Montell, manuscript submitted for publication).

The ERG and Retinal Degeneration Phenotypes Can Be Separated Suggesting Multiple Roles for p174 in the Rhabdomeres

We found that deletion of the kinase domain resulted in an ERG phenotype without retinal degeneration while two ts transformants, P[$ninaC^{366R}$] and P[$ninaC^{968.2}$], displayed only an ERG phenotype at the nonpermissive temperature (Table I). These results indicate that neither the ERG nor the retinal degeneration phenotypes is a secondary effect of the other. Furthermore, the more severe ERG phenotype associated with P[$ninaC^{MD}$] than with P[$ninaC^{KD}$] discussed above was unlikely to be a secondary effect of retinal degeneration since P[$ninaC^{366R}$] and P[$ninaC^{968.2}$] exhibited retinal degeneration at the nonpermissive temperature without affecting the ERG.

The results demonstrating that the *ninaC* retinal degeneration and ERG phenotypes are not obligatorily coupled suggest that p174 has multiple functions. In addition to a role

in phototransduction discussed above, p174 might also serve a structural role since the retinal degeneration appears to be unrelated to the defective ERG (Fig. 9 *B*). It is possible that p174 might serve to link the actin filaments in the rhabdomeres to the membrane as has been proposed for the intestinal brush border myosin I (reviewed in Pollard et al., 1991; Chenev and Mooseker, 1992). The p174 could bind directly to the rhabdomeral membrane via the myosin I-like tail domain or serve to link the actin filaments to a membrane protein. A number of proteins, such as dystrophin, have been described which bridge actin filaments with the plasma membrane and are required to maintain the integrity of the cell (reviewed in Luna and Hitt, 1992). Disruption of either the putative actin- or membrane-binding activities of NINAC might disrupt the membrane-actin link and lead to degeneration of the rhabdomeres.

Temperature-sensitive Mutations May Identify Residues That Disrupt but Do Not Eliminate Functions of Myosins in General

The two ts mutations in *ninaC*, which cause retinal degeneration but do not affect the ERG, may be useful mutations to analyze, in other myosins, in order to obtain partial or temperature sensitive phenotypes. The glycine to arginine change in residue 366 in P[$ninaC^{366R}$] was the same mutation which caused a partial, but not temperature sensitive, phenotype in the EMS induced *unc-54* allele, s95 (Dibb et al., 1985). Due to the proximity to the ATP-binding site, the mutation in P[$ninaC^{366R}$] might perturb ATP binding. The other ts transformant, P[$ninaC^{968.2}$], contained mutations in residues which did not correspond to a known hypomorphic allele in *unc-54*. The alterations in P[$ninaC^{968.2}$] might interfere with optimal actin or light chain/calmodulin binding. The residues mutated in P[$ninaC^{366R}$] and P[$ninaC^{968.2}$] are conserved in all myosin head domains that have been sequenced. This suggests that these amino acids are important for function and that disruption of these residues might give rise to partial phenotypes in myosins other than UNC-54 and NINAC.

Concluding Remarks

Our working model for NINAC p174 function is that the role of the kinase domain is to regulate the activity of other rhabdomeric proteins important in phototransduction by serine/threonine phosphorylation (Fig. 9, *A* and *B*). We propose that the myosin domain has three functions: the first is to transport the linked kinase domain into the rhabdomeres so that it can access its rhabdomeric substrates; a second is to maintain the structure of the rhabdomere during periods of illumination; and a third role may be to carry another unlinked protein important in phototransduction into the rhabdomeres. Preliminary evidence indicates that the unlinked protein may be calmodulin (Porter, J. A., M. Yu, S. K. Doberstein, T. D. Pollard, and C. Montell, manuscript submitted for publication).

We thank S. K. Doberstein and Drs. D. J. Montell, P. N. Devreotes, and P. A. Beachy for helpful comments on this manuscript and T. Oyebade, A. Thomas and J. Li for technical assistance.

This investigation was supported by a grant from the National Eye Institute to C. Montell (EY08117). C. Montell also thanks the National Science Foundation for a Presidential Young Investigator Award and the American Cancer Society for a Junior Faculty Research Award.

Received for publication 29 January 1993 and in revised form 20 April 1993.

References

Aota, S., T. Gojobori, F. Ishibashi, T. Maruyama, and T. Ikemura. 1988. Codon usage tabulated from the GenBank sequence data. *Nucleic Acids Res.* 16 (supplement):r315-r316.

Assad, J. A., and D. P. Corey. 1992. An active motor model for adaptation by vertebrate hair cells. *J. Neurosci.* 12:3291-3309.

Blest, A. D. 1988. The turnover of phototransductive membrane in compound eyes. *In* Advances in Insect Physiology. P. D. Evans and V. B. Wigglesworth, editors. Academic Press, London. 1-54.

Buchner, E. 1991. Genes expressed in the adult brain of Drosophila and effects of their mutations on behavior: a survey of transmitter- and second messenger-related genes. *J. Neurogenet.* 7:153-192.

Cheney, R. E., and M. S. Mooseker. 1992. Unconventional myosins. *Curr. Op. Cell Biol.* 4:27-35.

Cohen, P. 1989. The structure and regulation of protein phosphatases. *Ann. Rev. Biochem.* 58:453-508.

Dibb, N. J., D. M. Brown, J. Karn, D. G. Moerman, S. L. Bolten, and R. H. Waterson. 1985. Sequence analysis of mutations that affect the synthesis, assembly and enzymatic activity of the *unc-54* myosin heavy chain of *Caenorhabditis elegans*. *J. Mol. Biol.* 183:543-551.

Doberstein, S. K., and T. D. Pollard. 1992. Localization and specificity of the phospholipid and actin binding sites on the tail of *Acanthamoeba* myosin IC. *J. Cell Biol.* 117:1241-1249.

Edelman, A. M., D. K. Blumenthal, and E. G. Kreb. 1987. Protein serine/threonine kinases. *Ann. Rev. Biochem.* 56:567-613.

Endow, S. A., and M. A. Titus. 1992. Genetic approaches to molecular motors. *Annu. Rev. Cell Biol.* 8:29-66.

Franceschini, N., and K. Kirschfeld. 1971. Les phénomènes de pseudopupille dans l'oeil composé de Drosophila. *Kybertik.* 9:159-182.

Fry, D. C., S. A. Kuby, and A. S. Mildvan. 1986. ATP-binding site of adenylate kinase: mechanistic implications of its homology with ras-encoded p21, F_1-ATPase, and other nucleotide-binding proteins. *Proc. Natl. Acad. Sci. USA.* 83:907-911.

Hicks, J. L., and D. S. Williams. 1992. Distribution of the myosin I-like *ninaC* proteins in the *Drosophila* retina and ultrastructural analysis of mutant phenotypes. *J. Cell Sci.* 101:247-254.

Hudspeth, A. J. 1989. How the ear's works work. *Nature (Lond.)* 341:397-404.

Knighton, D. R., J. H. Zheng, L. F. Ten Eyck, V. A. Ashford, N. H. Xuong, and S. S. Taylor. 1991. Crystal structure of the catalytic subunit of cyclic adenosine monophosphate-dependent protein kinase. *Science (Wash. DC).* 253:407-414.

Korn, E. D., and J. A. Hammer, III. 1988. Myosins of nonmuscle cells. *Ann. Rev Biophys. Biophys. Chem.* 17:23-45.

Luna, E. J., and A. L. Hitt. 1992. Cytoskeleton-plasma membrane interactions. *Science (Wash. DC)* 258:955-964.

Matsumoto, H., and W. L. Pak. 1984. Light-induced phosphorylation of retina-specific polypeptides or *Drosophila* in vivo. *Science (Wash. DC).* 223: 184-186.

Matsumoto, H., K. Isono, Q. Pye, and W. L. Pak. 1987. Gene encoding cytoskeletal proteins in Drosophila rhabdomeres. *Proc. Natl. Acad. Sci. USA.* 84:985-989.

Mismer, D., and G. M. Rubin. 1987. Analysis of the promoter of the *ninaE* opsin gene in Drosophila melanogaster. *Genetics.* 116:565-578.

Montell, C., and G. M. Rubin. 1988. The Drosophila *ninaC* locus encodes two photoreceptor cell specific proteins with domains homologous to protein kinases and the myosin heavy chain head. *Cell.* 52:757-772.

Norbury, C., and P. Nurse. 1992. Animal cell cycles and their control. *Ann. Rev. Biochem.* 61:441-470.

Pollard, T. D. 1984. Purification of a high molecular weight actin filament gelation protein from *Acanthamoeba* that shares antigenic determinants with vertebrate spectrins. *J. Cell Biol.* 99:1970-1980.

Pollard, T. D., S. K. Doberstein, and H. G. Zot. 1991. Myosin-I. *Annu. Rev. Physiol.* 53:653-681.

Porter, J. A., J. L. Hicks, D. S. Williams, and C. Montell. 1992. Differential localizations of and requirements for the two Drosophila *ninaC* kinase/myosins in photoreceptor cells. *J. Cell Biol.* 116:683-693.

Rubin, G. M., and A. C. Spradling. 1982. Genetic transformation of Drosophila with transposable element vectors. *Science (Wash. DC).* 218:348-353.

Spradling, A. C., and G. M. Rubin. 1982. Transposition of cloned P elements into Drosophila germline chromosomes. *Science (Wash. DC).* 218:341-347.

Spudich, J. A. 1989. In pursuit of myosin function. *Cell Regul.* 1:1-11.

Tan, J. L., S. Ravid, and J. A. Spudich. 1992. Control of nonmuscle myosins by phosphorylation. *Ann. Rev. Biochem.* 61:721-759.

Warrick, H. M., and J. A. Spudich. 1987. Myosin structure and function in cell motility. *Annu. Rev. Cell Biol.* 3:379-421.